applied nano

MDPI

Communication

Green Synthesis of Magnetic Fe–Co Bimetallic Nanoparticles and Their Photocatalytic Activity

Amit Bhardwaj and Arun K. Singh *

Department of Chemistry, M. M. Engineering College, Maharishi Markandeshwar (Deemed to be University), Mullana, Ambala, Haryana 133207, India
* Correspondence: aruniitr09@gmail.com

Abstract: The leaves of the *Murraya koenigii* aromatic plant contain various specific phytochemicals, including lutein, β-carotene, vitamin C, nicotinic acids, and other polyphenols, which act as reducing agents to produce metallic nanoparticles from their respective precursors. In this study, we report the green synthesis of iron–cobalt bimetallic nanoparticles (Fe–Co BMNPs) using natural resources of reducing and capping agents from aqueous extract of *Murraya koenigii* leaves. The synthesized Fe–Co BMNPs were characterized using SEM, EDS, BET surface area, TGA, XRD, TEM, and VSM techniques, revealing their crystalline structure with a surface area of 83.22 m^2 g^{-1} and particle sizes <50 nm. Furthermore, the photocatalytic ability of the synthesized Fe–Co BMNPs was examined concerning methylene blue dye (MBD) aqueous solution. The synthesized Fe–Co BMNPs exhibited promising potential for dye removal from aqueous solution in acidic and basic medium (>97% of 10 mg L^{-1}).

Keywords: bimetallic nanoparticles; green synthesis; photocatalytic activity

Citation: Bhardwaj, A.; Singh, A.K. Green Synthesis of Magnetic Fe–Co Bimetallic Nanoparticles and Their Photocatalytic Activity. *Appl. Nano* **2024**, *5*, 108–115. https://doi.org/10.3390/applnano5030009

Academic Editors: Giulio Malucelli and Michalis Konsolakis

Received: 13 April 2024
Revised: 8 June 2024
Accepted: 11 July 2024
Published: 30 July 2024

1. Introduction

Dyes are widely used as raw materials in various applications including paper and textile industries. For instance, methylene blue dye (MBD) bearing an aromatic ring is a cationic thiazine dye used to color silk, wool, cotton, etc. [1]. Moreover, MBD is water-soluble, carcinogenic, non-biodegradable, and resistant to light and temperature in water [1]. Its inhalation causes respiratory problems [2]. Thus, MBD-contaminated water is a severe threat to the aquatic ecosystem and human beings' health [1]. Among various reported techniques for treating dye-contaminated water, photocatalysis based on metal oxide nanoparticles has attracted significant attention because of the optoelectronic properties, chemical stability, and ability to generate e^-/h^+ pairs based on species very reactive to degrade dyes [3,4]. Metal oxides such as cobalt oxide nanoparticles are useful in diverse applications, including photocatalysis, sensing, medical, and electrical devices [4–6]. The specific properties such as high surface area, favorable band gap, multivalent oxidation states, and catalytic ability make them attractive transition metal nanoparticles [5]. Several methods, such as sol–gel, sonochemical, thermal decomposition, laser ablation, hydrothermal, co-precipitation, and green synthesis, have been reported in the literature to synthesize cobalt nanoparticles [5,7–9]. Among these, the plant-extract-mediated green approach provides several advantages for iron and cobalt nanoparticle synthesis compared to other methods, such as being simple, inexpensive, eco-friendly, non-toxic, versatile, and cost-effective [9–11]. The plant-extract-mediated green synthesis approach eliminated the requirement of reducing and stabilizing chemical agents during the synthesis of nanoparticles from their respective metal ion precursors [12,13]. The specific biomolecules in plant extracts, such as polyphenols, flavonoids, and alkaloids, act as good reducing and stabilizing agents for synthesizing stable metallic nanoparticles [14]. For instance, Vinyagam et al. [5] reported cobalt oxide nanoparticle synthesis using *Muntingia calabura* leaf extract and the synthesized nanoparticles' photocatalytic ability was examined

for dye-contaminated water under natural sunlight irradiation. The prepared nanoparticles showed significant photocatalytic activity with a specific surface area of 10.31 m^2 g^{-1} and particle size of 27.59 nm. Shanmuganathan et al. [15] reported cobalt oxide nanoparticle synthesis via a green approach using *Curcuma longa* root extract. SEM, XRD, and DLS analysis confirmed the formation of spherical, crystalline cobalt oxide nanoparticles with an average size distribution of 97.5 ± 35.1 nm. In addition, synthesized nanoparticles exhibited excellent photocatalytic degradation of methyl orange, methyl red, and methyl blue dye in aqueous solution along with antifungal, antibacterial, and antioxidant activity. Nevertheless, metallic nanoparticles alone as a catalyst or an adsorbent also have limitations. For instance, metallic nanoparticles are very small in size (<100 nm). Thus, during their application in dye degradation from contaminated water, there is greater chance of secondary contamination by nanoparticles because of the insufficient recovery of metallic nanoparticles from treated water [16]. Therefore, effective and easily separable metallic nanoparticles are highly essential for the remediation of contaminated water without the creation of secondary pollution. Considering the advantages of the plant-mediated green synthesis approach and need for an easily separable photocatalyst, iron–cobalt bimetallic nanoparticles (Fe–Co BMNPs) were prepared using the extract of *Murraya koenigii* leaf. Bimetallic nanoparticles are attracting more attention for catalytic reactions [17,18]. The combination of iron along with the cobalt nanoparticles can provide better separation ability from treated water along with catalytic/adsorption ability [19,20]. *Murraya koenigii* (curry leaves) is a commonly available medicinal plant with various bioactive compounds such as flavonoids, essential oils, alkaloids, carotene, nicotinic acids, and a high content of oxalic acids [21,22]. In recent years, green synthesis of various metallic nanoparticles (Fe, Cu, Zn, Ag, etc.) has been reported using extract of curry leaves [21,23,24]. However, magnetically recoverable green synthesis of Fe–Co BMNPs (surface area of 83.22 m^2 g^{-1} and saturation magnetization value of 28.38 emu g^{-1}) has not been attempted yet using *Murraya koenigii* leaf extract. The photocatalytic dye degradation ability of the synthesized Fe–Co BMNPs was examined for removal of MBD from aqueous solution.

2. Materials and Methods

2.1. Materials

Cobalt nitrate (>96%) was purchased from Molychem. Ferrous chloride (>99%) was purchased from Molychem. Sodium hydroxide (pellets, ≥75%) and hydrochloric acid (HCl, ≥35%) were purchased from Loba Chemie. All the chemicals were used as received without further purification. Deionized (DI) water (18 MΩ) prepared all aqueous solutions. *Murraya koenigii* plant's leaves were collected at the university's campus (MM(DU), Mullana, Ambala) and washed 3–5 times with DI water.

2.2. Procedures for Preparation of Fe–Co BMNPs

2.2.1. Preparation of *Murraya koenigii* Plant Leaves Aqueous Extract

A total of 25 g of *Murraya koenigii* plant leaves was converted into small pieces by grinding, added to a beaker containing 100 mL DI water, and heated to boil at 80 °C for 1–2 h. The resultant extract was cooled, filtered via Whatman filter paper and stored in a clean glass vial for Fe–Co BMNPs synthesis [23].

2.2.2. Synthesis of Fe–Co BMNPs Using *Murraya koenigii* Plant Leaf Extract

Initially, 50 mL of aqueous leaf extract was heated at 80 °C with stirring on a magnetic stirrer [22,23]. Cobalt nitrate and ferrous chloride (0.5 M of each) were added to the heated aqueous extract, and the pH of the resulting solution was adjusted to approximately 11 by the appropriate addition of 1 M aqueous solution of NaOH. The heating process of this solution was continued along with stirring to form a dense product. The obtained viscous product was subjected to calcination at 400 °C for 2 h in a furnace (muffle). The resultant product of calcination process was washed several times using ethanol and water and then dried (Figure 1).

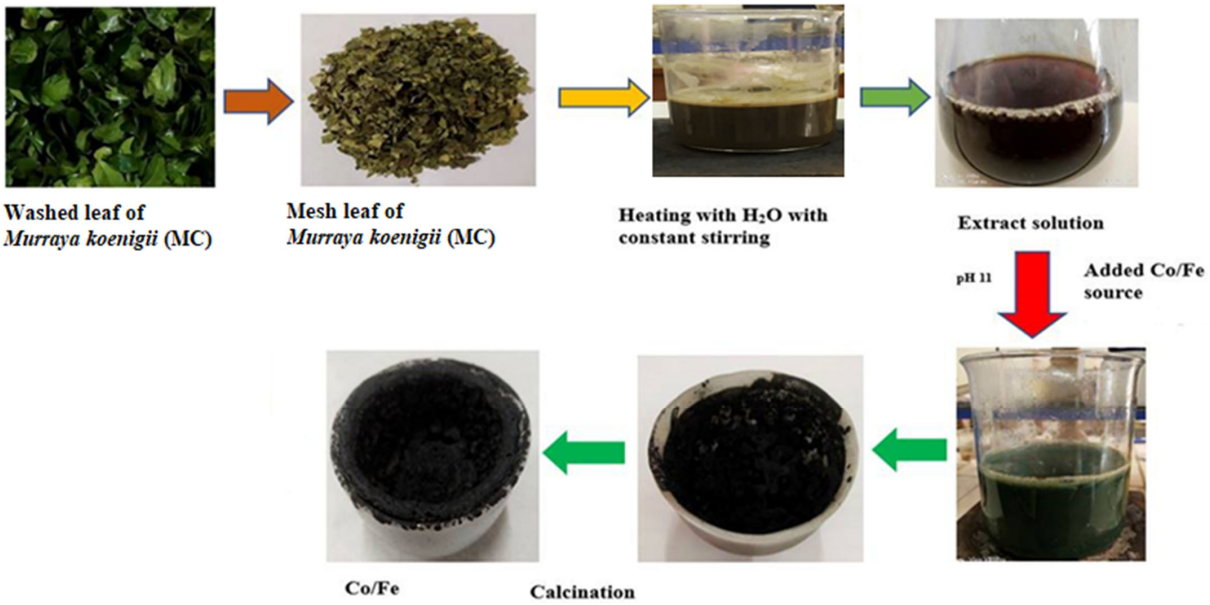

Figure 1. Schematic illustration for synthesizing Fe–Co BMNPs using aqueous extract of *Murraya koenigii* plant leaves.

2.3. Characterization of Synthesized Fe–Co BMNPs

Fe–Co BMNPs were characterized using a Scanning Electron Microscope (SEM) and energy-dispersive X-ray spectroscopy (EDS), respectively, for the analysis of morphological structure and elemental composition. The XRD (X-ray diffractometer) instrument was used for sample pattern recording from 10° to 80° at a scanning speed of 2°, 2θ per min. TGA (SII 6300 EXSTAR) analysis was performed (under N_2 atmosphere) to assess the thermal stability of the Fe–Co BMNPs at a heating rate of 10 °C min^{-1}. The particle size ranges of the synthesized Fe–Co BMNPs were determined through transmission electron microscopy (TEM; JEOL, JEM–1400).

The Quantachrome (BET method, Quantachrome, NOVA, 2200e, Boynton Beach, FL, USA) and VSM instruments (Make: Lakeshore, Model: 7410 series VSM system, Westerville, OH, USA) with magnetic fields were employed to analyze the surface area and magnetic properties of the synthesized Fe–Co based material, respectively [25,26].

2.4. Photocatalytic Ability of Fe–Co BMNPs

The dye degradation activity (photocatalytically) of the synthesized Fe–Co BMNPs was evaluated with the use of MBD in aqueous solution and natural sunlight exposure. In this experiment, 10 mL of 10 mg L^{-1} MBD aqueous solution was taken in separate glass vials, and 25 mg of Fe–Co BMNPs were added in each vial and placed in dark for adsorption–desorption equilibrium (30 min). Later, the resultant suspension was subjected to sunlight exposure (in an open atmosphere). At definite intervals (0, 30, 60, 90, 120, and 135 min, etc.), equilibrated samples were collected and Fe–Co BMNPs were separated using a simple magnet, because of their magnetic properties. The final MBD concentration in each separated samples was determined using an ultraviolet–visible spectrophotometer (Spectramax ID3, Molecular Devices, LLC., San Jose, CA, USA) at room temperature in the scanning range of 350 nm to 700 nm. The pH of the aqueous MBD solution was maintained in acidic (4.0) and basic (9.0) medium in order to assess the effect of pH during the photocatalytic dye degradation study.

3. Results and Discussion

The surface morphology, elemental composition, and crystallinity of the synthesized Fe–Co BMNPs were examined using FESEM, EDS, and X-ray diffractometer analysis (XRD patterns). The Fe–Co BMNPs SEM image (Figure 2a) demonstrates the irregular and rough

morphology appearance. The extent of aggregation may be due to the interaction with the phytochemicals of plant extract (hydrogen bonding), resulting in magnetostatic interaction (high surface energy of the nanoparticles) [5,27]. Figure 2b shows the EDS spectra of the synthesized Fe–Co BMNPs acquired from different portions of the synthesized nanoparticles. The obtained spectrum displays the peak area of Fe, Co, O, and C in the analyzed samples. The high signal and strong peak of 38.74% for Fe, 21.23% for Co, and 29.35% for O indicate the presence of Co and Fe in the form of oxide as main components of the synthesized materials. The obtained X-ray diffraction pattern from the X-ray diffractometer is expressed in Figure 2c. The crystalline phase of iron and cobalt oxides was identified. The appearance of strong peaks (2θ = 28.54, 33.06, 47.48, 56.32, 58.98,69.28, and 76.60) in the XRD pattern confirmed the crystallinity and high purity of the iron and cobalt oxide in the synthesized Fe–Co BMNPs [5,28,29]. The observed XRD pattern is similar to those obtained for cobalt iron oxide nanoparticles already reported in the literature [30,31]. It can be seen that >94% weight remains constant even after exposure to temperatures up to 800 °C. The Fe–Co BMNPs' TGA curve is shown in Figure 2d. The observed small reduction in their mass may be due to moisture (water molecules) evaporation into a gaseous state as well as the combustion of organic molecules [32,33]. This observation inferred the high thermal stability of Fe–Co BMNPs. TEM image analysis shows the average particle size of the synthesized Fe–Co BMNPs was below 50 nm (Figure 3a,b). The plot of magnetization (M) and magnetic field (Figure 3c) shows a 28.38 emu g^{-1} value of saturation magnetization (Ms). The Ms value is a key factor used to represent the magnetic strength of the prepared particles from the liquid phase (during separation of treated water) via simple external magnet [34]. This observed high value of Ms indicates that the prepared Fe–Co BMNPs possess magnetism and could be easily separated from the liquid phase with the help of a simple conventional magnet [26]. In addition, BET surface area was also measured via a N_2 adsorption–desorption isotherm (Figure 3d) [35]. The specific surface area was found to be 83.22 m^2 g^{-1}. The large surface area of the metallic nanoparticles is favorable to facilitate the higher active sites for catalytic reaction or sorption of water contaminants [13,30,36,37].

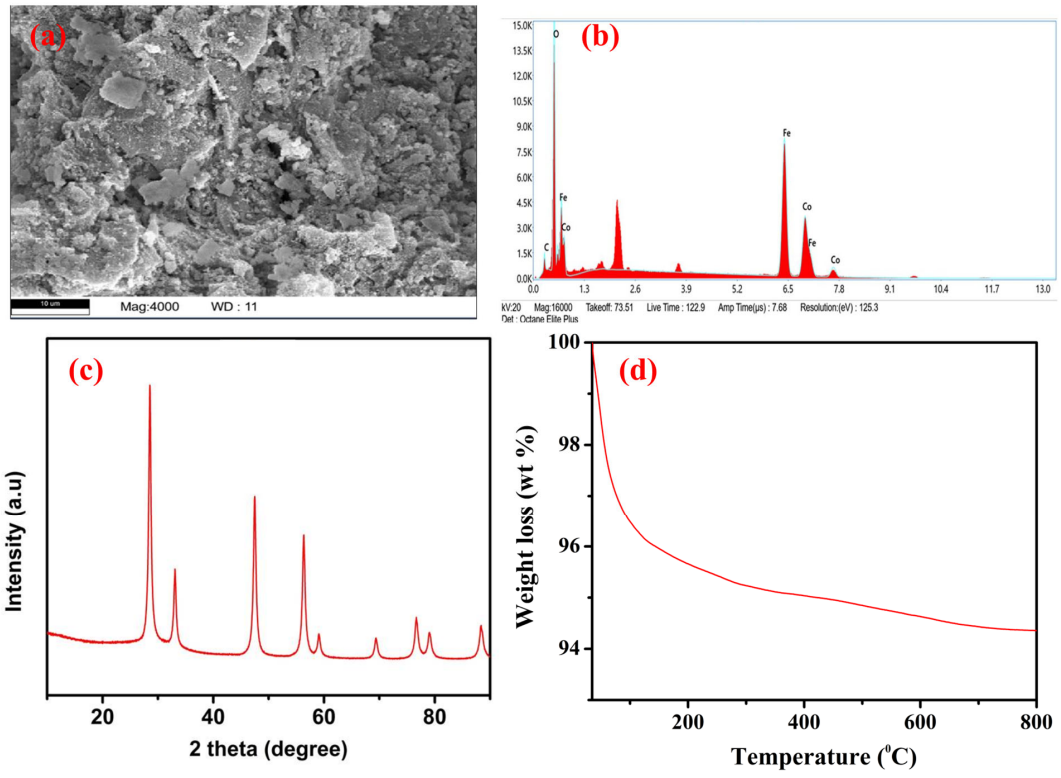

Figure 2. (**a**) Scanning electron microscopy (FESEM) image, (**b**) EDX analysis spectra, (**c**) X-ray diffraction (XRD) patterns, and (**d**) thermo gravimetric analysis (TGA) curve of the synthesized Fe–Co BMNPs.

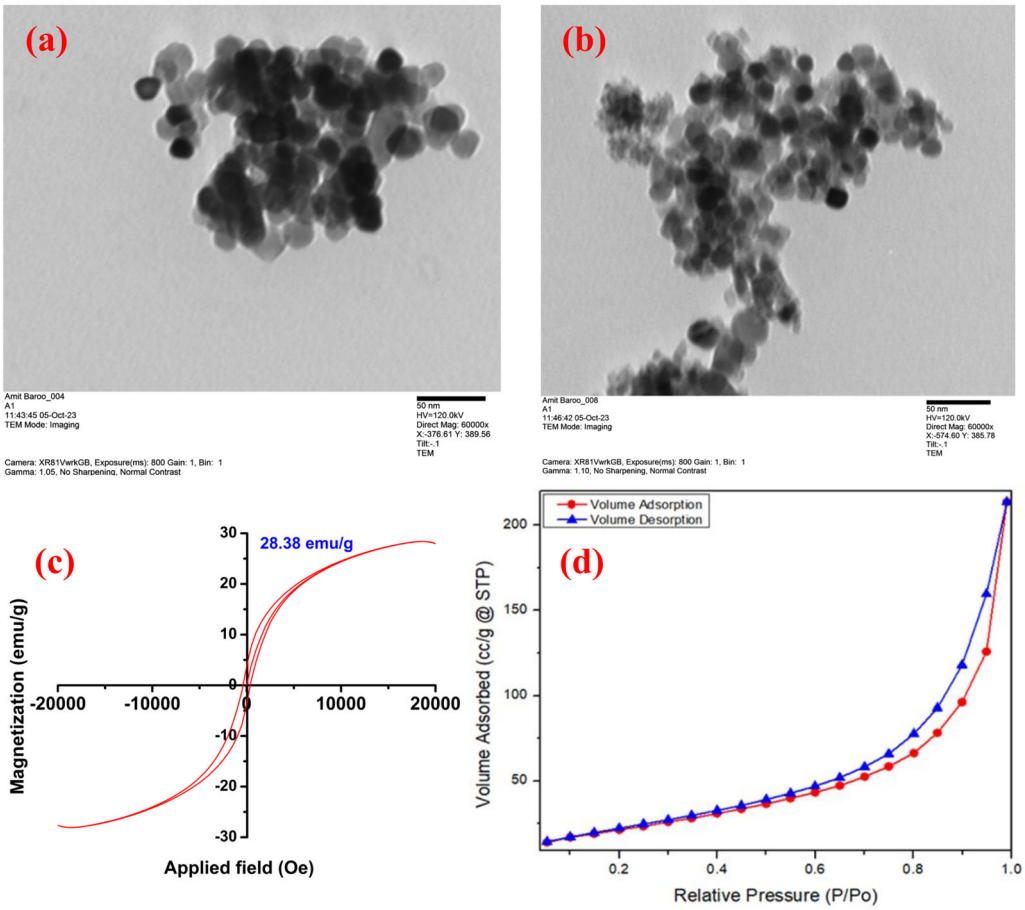

Figure 3. (**a**,**b**) Transmission electron microscopy (TEM) images, (**c**) VSM curve under the influence of the magnetic field, and (**d**) the adsorption–desorption isotherm during BET surface area analysis of the synthesized Fe–Co BMNPs.

The photocatalytic dye removal activity of the synthesized Fe–Co BMNPs was evaluated under natural sunlight exposure by observing UV–Vis absorption spectra. The blue dye color disappeared within a certain period when 25 mg and 50 mg Fe–Co BMNPs were added separately in the 10 mg L^{-1} MBD aqueous solution with a pH value of 4.0. Figure 4a,b depicts the absorbance spectra of changes in absorbance value (in the range of wavelength from 400 to 800 nm) for residual MBD concentration for different intervals of time (0, 30, 60, 90, 120, and 135 min, etc.) of sunlight exposure. The wavelength of 664 nm was observed as the lambda max of MBD aqueous solution [38,39]. Interestingly, it was also observed that the degradation efficacy of Fe–Co BMNPs was further increased when the pH of the MBD (concentration = 10 mg L^{-1}) aqueous solution was kept higher at approximately 9.0 (as depicted in Figure 4c,d).

At the pH of 9.0 of aqueous solution, the blue color of MBD was found to approximately disappear with an efficiency of 97% over 135 min and confirmed the effective catalytic activity for degradation of dye molecules. With the possibility of the higher number of adsorptive/reactive sites on the surface Fe–Co BMNPs with large surface area (83.22 m^2 g^{-1}), a moderate band gap and the formation of photo-generated electron–hole pairs at the hetero-junction surface may be the main reasons for MBD degradation in the presence of sunlight with high efficiency [36,40–42]. MBD is a cationic dye. The higher pH of the solution favors the electrostatic attraction between cationic MBD and the photocatalyst surface and enhances the generation of reactive oxygen species by photon-induced electron-hole pairs [9,40].

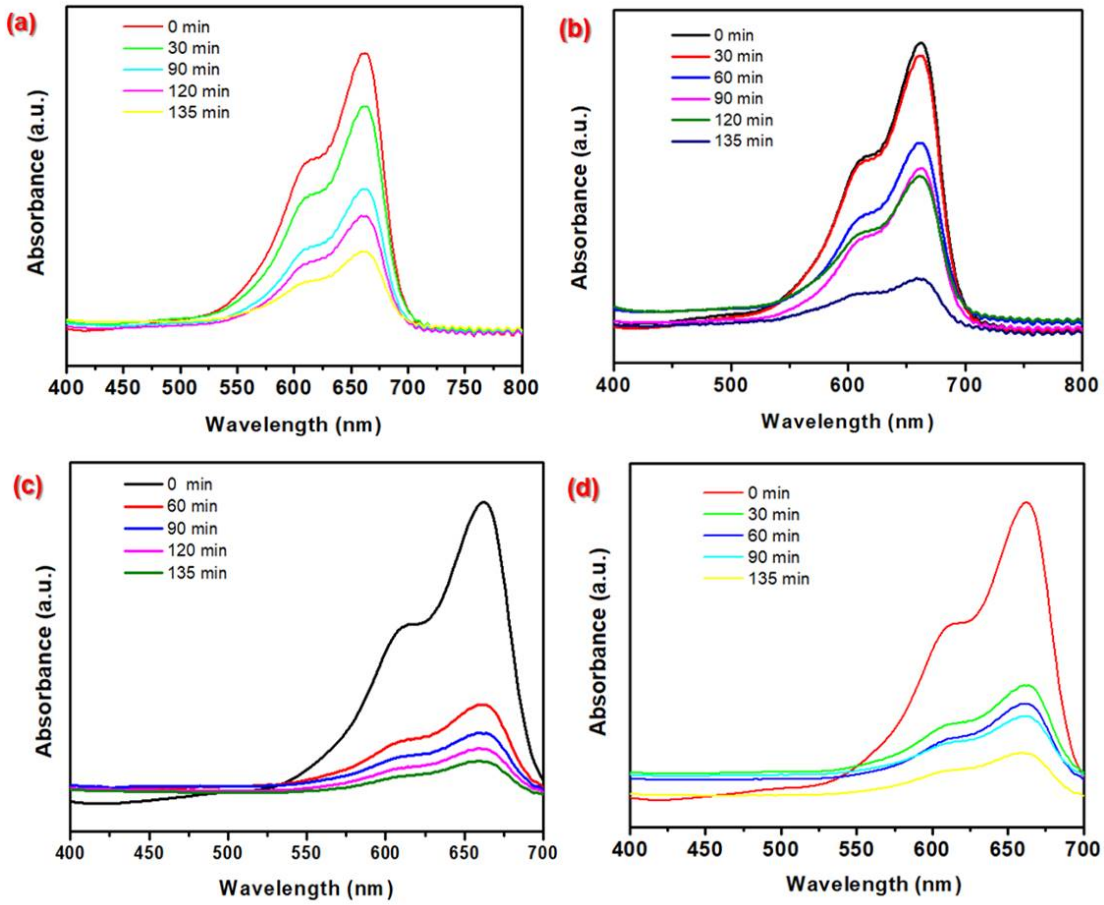

Figure 4. The temporal absorbance curves for MBD aqueous solution (conc. = 10 mg L^{-1}) before and after treatment with (**a**) 25 mg Fe–Co BMNP dose at pH = 4.0, (**b**) 50 mg Fe–Co BMNP dose at pH = 4.0, (**c**) 25 mg Fe–Co BMNP dose at pH = 9.0, and (**d**) 50 mg Fe–Co BMNP dose at pH = 9.0 during the photodegradation process under sunlight exposure.

4. Conclusions

This study reported the *Murraya koenigii* leaf-extract-mediated green synthesis of magnetically separable Fe–Co BMNPs. The results of characterization analysis using XRD pattern, VSM, and SEM-EDS revealed the formation of the crystalline structure of Fe–Co BMNPs with the major components of Fe (38.74%), Co (21.23%), oxygen (29.35%), and a saturation magnetization value of 28.38 emu g^{-1}. Furthermore, results of photocatalytic analysis inferred that the Fe–Co BMNPs degraded >97% of 10 mg L^{-1} MBD within 135 min of exposure to sunlight. Thus, the study's results confirmed the efficient photocatalytic activity of the Fe–Co BMNPs.

5. Patents

The "preparation methodology of magnetic Fe–Co bimetallic photocatalyst" described in this study is subject of the Indian patent application number: 202411028940.

Author Contributions: Conceptualization, methodology, formal analysis, investigation, resources, data curation, writing—original draft preparation, writing—review and editing, supervision, A.K.S.; Experiments and data analysis, A.B. All authors have read and agreed to the published version of the manuscript.

Funding: This research received no external funding.

Institutional Review Board Statement: Not applicable.

Informed Consent Statement: Not applicable.

Data Availability Statement: The raw data supporting the conclusions of this article will be made available by the authors on request.

Acknowledgments: The authors acknowledge the support from the Department of Chemistry and Research & Development Cell of Maharishi Markandeshwar (Deemed to be University), Mullana, Ambala, Haryana, India.

Conflicts of Interest: The authors declare no conflicts of interest.

References

1. Kumar, G.; Dutta, R.K. Sunlight mediated photo-Fenton degradation of tetracycline antibiotic and methylene blue dye in aqueous medium using $FeWO_4/Bi_2MoO_6$ nanocomposite. *Process Saf. Environ. Prot.* **2022**, *159*, 862–873. [CrossRef]
2. Aaddouz, M.; Azzaoui, K.; Akartasse, N.; Mejdoubi, E.; Hammouti, B.; Taleb, M.; Sabbahi, R.; Alshahateet, S.F. Removal of methylene blue from aqueous solution by adsorption onto hydroxyapatite nanoparticles. *J. Mol. Struct.* **2023**, *1288*, 135807. [CrossRef]
3. Verma, V.; Singh, S.V. Augmentation of photocatalytic degradation of methylene blue dye using lanthanum and iodine Co-doped TiO_2 nanoparticles, their regeneration and reuse; and preliminary phytotoxicity studies for potential use of treated water. *J. Environ. Chem. Eng.* **2023**, *11*, 111339. [CrossRef]
4. Singh, A.K. A review on plant extract-based route for synthesis of cobalt nanoparticles: Photocatalytic, electrochemical sensing and antibacterial applications. *Curr. Res. Green Sustain. Chem.* **2022**, *5*, 100270. [CrossRef]
5. Vinayagam, R.; Hebbar, A.; Kumar, P.S.; Rangasamy, G.; Varadavenkatesan, T.; Murugesan, G.; Srivastava, S.; Goveas, L.C.; Kumar, N.M.; Selvaraj, R. Green synthesized cobalt oxide nanoparticles with photocatalytic activity towards dye removal. *Environ. Res.* **2023**, *216*, 114766. [CrossRef] [PubMed]
6. Shang, J.; Ma, C.; Zhang, C.; Zhang, W.; Shen, B.; Wang, F.; Guo, S.; Yao, S. Separator Modified by Carbon-Encapsulated CoFe Alloy Nanoparticles Supported on Carbon Nanotubes for Advanced Lithium-Sulfur Batteries. *ACS Appl. Nano Mater.* **2023**, *7*, 1786–1796. [CrossRef]
7. Babu, G.A.; Ravi, G.; Hayakawa, Y.; Kumaresavanji, M. Synthesis and calcinations effects on size analysis of Co_3O_4 nanospheres and their superparamagnetic behaviors. *J. Magn. Magn. Mater.* **2015**, *375*, 184–193. [CrossRef]
8. Adekunle, A.S.; Oyekunle, J.A.O.; Durosinmi, L.M.; Oluwafemi, O.S.; Olayanju, D.S.; Akinola, A.S.; Obisesan, O.R.; Akinyele, O.F.; Ajayeoba, T.A. Potential of cobalt and cobalt oxide nanoparticles as nanocatalyst towards dyes degradation in wastewater. *Nano-Struct. Nano-Objects* **2020**, *21*, 100405. [CrossRef]
9. Dey, C.; Nandi, M.; Goswami, M.M. pH dependent enhanced synchronous photocatalytic removal of cationic and anionic dyes by $CoFe_2O_4$ magnetic nanoparticles. *J. Mol. Struct.* **2023**, *1277*, 134859. [CrossRef]
10. Kumar, V.; Kaushik, N.K.; Tiwari, S.K.; Singh, D.; Singh, B. Green synthesis of iron nanoparticles: Sources and multifarious biotechnological applications. *Int. J. Biol. Macromol.* **2023**, *253*, 127017. [CrossRef]
11. Fiaz, S.; Ahmed, M.N.; Haq, I.U.; Shah, S.W.A.; Waseem, M. Green synthesis of cobalt ferrite and Mn doped cobalt ferrite nanoparticles: Anticancer, antidiabetic and antibacterial studies. *J. Trace Elem. Med. Biol.* **2023**, *80*, 127292. [CrossRef] [PubMed]
12. Singh, A.K. Flower extract-mediated green synthesis of bimetallic Cu[sbnd]Zn oxide nanoparticles and its antimicrobial efficacy in hydrocolloid films. *Bioresour. Technol. Rep.* **2022**, *18*, 101034. [CrossRef]
13. Singh, A.K. Ocimum sanctum mediated phytosynthesis of metallic nanoparticles: A review. *Bioresour. Technol. Rep.* **2022**, *19*, 101118. [CrossRef]
14. Malik, M.A.; Alshehri, A.A.; Patel, R. Facile one-pot green synthesis of Ag-Fe bimetallic nanoparticles and their catalytic capability for 4-nitrophenol reduction. *J. Mater. Res. Technol.* **2021**, *12*, 455–470. [CrossRef]
15. Shanmuganathan, R.; Sathiyavimal, S.; Le, Q.H.; Al-Ansari, M.M.; Al-Humaid, L.A.; Jhanani, G.K.; Lee, J.; Barathi, S. Green synthesized Cobalt oxide nanoparticles using Curcuma longa for anti-oxidant, antimicrobial, dye degradation and anti-cancer property. *Environ. Res.* **2023**, *236*, 116747. [CrossRef]
16. Munagapati, V.S.; Wen, H.Y.; Gollakota, A.R.K.; Wen, J.C.; Lin, K.Y.A.; Shu, C.M.; Yarramuthi, V.; Basivi, P.K.; Reddy, G.M.; Zyryanov, G.V. Magnetic Fe_3O_4 nanoparticles loaded guava leaves powder impregnated into calcium alginate hydrogel beads (Fe_3O_4-GLP@CAB) for efficient removal of methylene blue dye from aqueous environment: Synthesis, characterization, and its adsorption performance. *Int. J. Biol. Macromol.* **2023**, *246*, 125675. [CrossRef] [PubMed]
17. Zhang, Y.; Huang, J.; Dong, Z.; Zhan, Y.; Xi, J.; Xiao, J.; Huang, S.; Tian, F. Pd–Fe bimetallic nanoparticles anchored on N-doped carbon-modified graphene for efficient catalytic organic reactions. *Carbon Lett.* **2023**, *33*, 77–87. [CrossRef]
18. Xi, J.; Wang, Q.; Duan, X.; Zhang, N.; Yu, J.; Sun, H.; Wang, S. Continuous flow reduction of organic dyes over Pd-Fe alloy based fibrous catalyst in a fixed-bed system. *Chem. Eng. Sci.* **2021**, *231*, 116303. [CrossRef]
19. Li, L.; Wu, H.; Chen, H.; Zhang, J.; Xu, X.; Wang, S.; Wang, S.; Sun, H. Heterogeneous activation of peroxymonosulfate by hierarchically porous cobalt/iron bimetallic oxide nanosheets for degradation of phenol solutions. *Chemosphere* **2020**, *256*, 127160. [CrossRef]
20. Iqbal, A.; Cevik, E.; Bozkurt, A.; Asiri, S.M.M.; Alagha, O.; Qahtan, T.F.; Jalees, M.I.; Farooq, M.U. Ultrahigh adsorption by regenerable iron-cobalt core-shell nanospheres and their synergetic effect on nanohybrid membranes for removal of malachite green dye. *J. Environ. Chem. Eng.* **2022**, *10*, 107968. [CrossRef]

21. Devadoss, D.; Asirvatham, A.; Kujur, A.; Saaron, G.; Devi, N.; Mary, S.J. Green synthesis of copper oxide nanoparticles from Murraya koenigii and its corrosion resistivity on Ti-6Al-4V dental alloy. *J. Mech. Behav. Biomed. Mater.* **2023**, *146*, 106080. [CrossRef] [PubMed]
22. Elamin, N.Y.; Indumathi, T.; Kumar, E.R. Murraya koenigii mediated synthesis of cobalt doped NiO nanoparticles: Evaluation of structural, optical properties and anti-bacterial activity. *Phys. E Low-Dimens. Syst. Nanostruct.* **2022**, *142*, 115295. [CrossRef]
23. Sarma, P.P.; Barman, K.; Baruah, P.K. Green synthesis of silver nanoparticles using *Murraya koenigii* leaf extract with efficient catalytic, antimicrobial, and sensing properties towards heavy metal ions. *Inorg. Chem. Commun.* **2023**, *152*, 110676. [CrossRef]
24. Selvan, D.S.A.; Kumar, R.S.; Murugesan, S.; Shobana, S.; Rahiman, A.K. Antidiabetic activity of phytosynthesized Ag/CuO nanocomposites using *Murraya koenigii* and *Zingiber officinale* extracts. *J. Drug Deliv. Sci. Technol.* **2022**, *67*, 102838. [CrossRef]
25. Parveen, M.F.; Ranchani, A.A.J.; Parthasarathy, V.; Anbarasan, R. Efficient catalytic application of Cu-Fe bimetallic nanoparticles towards the preparation of bio-medically important polymer based Schiff bases. *Surf. Interfaces* **2021**, *25*, 101197. [CrossRef]
26. Singh, K.P.; Singh, A.K.; Singh, U.V.; Verma, P. Optimizing removal of ibuprofen from water by magnetic nanocomposite using Box-Behnken design. *Environ. Sci. Pollut. Res.* **2012**, *19*, 724–738. [CrossRef] [PubMed]
27. Ghorbani, H.; Eshraghi, M.; Dodaran, A.A.S. Structural and magnetic properties of cobalt ferrite nanoparticles doped with cadmium. *Phys. B Condens. Matter.* **2022**, *634*, 413816. [CrossRef]
28. Yonti, C.N.; Tsobnang, P.K.; Fomekong, R.L.; Devred, F.; Mignolet, E.; Larondelle, Y.; Hermans, S.; Delcorte, A.; Ngolui, J.L. Green synthesis of iron-doped cobalt oxide nanoparticles from palm kernel oil via co-precipitation and structural characterization. *Nanomaterials* **2021**, *11*, 2833. [CrossRef] [PubMed]
29. Xiang, D.; Lu, S.; Ma, Y.; Zhao, L. Synergistic photocatalysis-fenton reaction of flower-shaped CeO_2/Fe_3O_4 magnetic catalyst for decolorization of high concentration congo red dye. *Colloids Surf. A Physicochem. Eng. Asp.* **2022**, *647*, 129021. [CrossRef]
30. Xu, H.; Bi, S.; Xue, M.; Zhou, W.; Zhang, C. Amorphous cobalt iron oxide nanoparticles with high magnetization intensity for spin conversion of hydrogen at 77K. *Int. J. Hydrogen Energy* **2023**, *48*, 31643–31652. [CrossRef]
31. Ribeiro, J.J.K.; Porto, P.S.S.; Proveti, J.R.C.; Pessoa, M.S.; Morais, P.C.; Moscon, P.S.; Pereira, R.D.; Muniz, E.P. Influence of orange residue content on Sol-gel synthesis of cobalt ferrite Nanoparticles: Morphological and magnetic properties. *J. Magn. Magn. Mater.* **2023**, *586*, 171220. [CrossRef]
32. Aalami, Z.; Hoseinzadeh, M.; Manesh, P.H.; Aalami, A.H.; Es'haghi, Z.; Darroudi, M.; Sahebkar, A.; Hosseini, H.A. Synthesis, characterization, and photocatalytic activities of green sol-gel ZnO nanoparticles using *Abelmoschus esculentus* and *Salvia officinalis*: A comparative study versus co-precipitation-synthesized nanoparticles. *Heliyon* **2024**, *10*, e24212. [CrossRef]
33. Singh, A.K.; Ketan, K.; Singh, J.K. Simple and green fabrication of recyclable magnetic highly hydrophobic sorbents derived from waste orange peels for removal of oil and organic solvents from water surface. *J. Environ. Chem. Eng.* **2017**, *5*, 5250–5259. [CrossRef]
34. Mabarroh, N.; Alfansuri, T.; Wibowo, N.A.; Istiqomah, N.I.; Tumbelaka, R.M.; Suharyadi, E. Detection of green-synthesized magnetite nanoparticles using spin-valve GMR-based sensor and their potential as magnetic labels. *J. Magn. Magn. Mater.* **2022**, *560*, 169645. [CrossRef]
35. Mahlaule-Glory, L.M.; Mathobela, S.; Hintsho-Mbita, N.C. Biosynthesized Bimetallic ($ZnOSnO_2$) Nanoparticles for Photocatalytic Degradation of Organic Dyes and Pharmaceutical Pollutants. *Catalysts* **2022**, *12*, 334. [CrossRef]
36. Bhardwaj, K.; Singh, A.K. Bio-waste and natural resource mediated eco-friendly synthesis of zinc oxide nanoparticles and their photocatalytic application against dyes contaminated water. *Chem. Eng. J. Adv.* **2023**, *16*, 100536. [CrossRef]
37. Singh, A.K.; Bhardwaj, K. Mechanistic understanding of green synthesized cerium oxide for the photocatalytic degradation of dyes and antibiotics from aqueous media and antimicrobial efficacy: A review. *Environ. Res.* **2023**, *246*, 118001. [CrossRef]
38. Shaheen, I.; Ata, S.; Aslam, H.; Farooq, H.; Ali, A.; Elqahtani, Z.M.; Alwadai, N.; Iqbal, M.; Arif, H.; Nazir, A. Photocatalytic removal of methylene blue and Victoria blue R dyes using Tb and La-doped $BaZnO_2$. *Desalin. Water Treat.* **2024**, *318*, 100389. [CrossRef]
39. Aldabagh, I.S.; Saad, D.N.; Ahmed, E.I. Removal of methylene blue from aqueous solution by green Synthesized silicon dioxide Nanoparticles using Sunflower Husk. *Chem. Eng. J. Adv.* **2024**, *18*, 100608. [CrossRef]
40. Intharaksa, O.; Nanan, S.; Patdhanagul, N.; Panphojan, T.; Srikakul, T.; Tantisuwichwong, N.; Tantisuwichwong, N.; Dulyasucharit, R. Preparation of magnetic $CuO/Fe_3O_4/ZnO$ photocatalyst for complete degradation of methylene blue under natural sunlight irradiation. *J. Phys. Chem. Solids* **2023**, *182*, 111577. [CrossRef]
41. Yang, X.; Zhao, J.; Cavaco-Paulo, A.; Su, J.; Wang, H. Encapsulated laccase in bimetallic Cu/Zn ZIFs as stable and reusable biocatalyst for decolorization of dye wastewater. *Int. J. Biol. Macromol.* **2023**, *233*, 123410. [CrossRef]
42. Riaz, T.; Assey, N.; Javed, M.; Shahzadi, T.; Zaib, M.; Shahid, S.; Iqbal, S.; Elkaeed, E.B.; Alzhrani, R.M.; Alsaab, H.O.; et al. Biogenic plant mediated synthesis of monometallic zinc and bimetallic Copper/Zinc nanoparticles and their dye adsorption and antioxidant studies. *Inorg. Chem. Commun.* **2022**, *140*, 109449. [CrossRef]